J Bioenerg Biomembr (2011) 43:507–518
DOI 10.1007/s10863-011-9375-2

Mitochondrial dysfunction and effect of antiglycolytic bromopyruvic acid in GL15 glioblastoma cells

Lara Macchioni · Magdalena Davidescu · Miriam Sciaccaluga · Cristina Marchetti · Graziella Migliorati · Stefano Coaccioli · Rita Roberti · Lanfranco Corazzi · Emilia Castigli

Received: 26 March 2011 / Accepted: 21 June 2011 / Published online: 21 July 2011

Abstract Most cancer cells, including GL15 glioblastoma cells, rely on glycolysis for energy supply. The effect of antiglycolytic bromopyruvate on respiratory parameters and viability of GL15 cells was investigated. Bromopyruvate caused $\Delta\psi_m$ and MTT collapse, ATP decrease, and cell viability loss without involving apoptotic or necrotic pathways. The autophagy marker LC3-II was increased. $\Delta\psi_m$ decrease was accompanied by reactive oxygen species (ROS) increase and cytochrome c (cyt c) disappearance, suggesting a link between free radical generation and intramitochondrial cyt c degradation. Indeed, the free radical inducer menadione caused a decrease in cyt c that was reversed by N-acetylcysteine. Cyt c is tightly bound to the inner mitochondrial membrane in GL15 cells, which may confer protein peroxidase activity, resulting in autooxidation and protein targeting to degradation in the presence of ROS. This process is directed towards impairment of the apoptotic cyt c cascade, although cells are committed to die.

Keywords GL15 cells · Cytochrome c · ROS · Mitochondrial membrane potential · Bromopyruvate · Respiratory chain inhibitors

Abbreviations

DMEM	Dulbecco's modified Eagle's medium
Cyt c	cytochrome c
HEPES	4-(2-hydroxyethyl)-1-piperazineethansulfonic acid
JC-1	5,5′,6,6′-tetrachloro-1,1′,3,3′-tetraethylbenzimidazolylcarbocyanine iodide
DHE	dihydroethidine
PI	propidium iodide
MTT	3-(4,5-dimethyl-thiazol-2-yl)-2,5-diphenyl tetrazolium bromide
CCCP	carbonyl cyanide 3-chlorophenylhydrazone
ROS	reactive oxygen species
$\Delta\psi_m$	mitochondrial membrane potential
IGFL	integral of mean fluorescence

L. Macchioni · M. Davidescu · S. Coaccioli · R. Roberti · L. Corazzi (✉)
Department of Internal Medicine,
University of Perugia,
Via del Giochetto,
06122 Perugia, Italy
e-mail: corazzi@unipg.it

M. Sciaccaluga
Istituto Pasteur-Fondazione Cenci Bolognetti and Department of Physiology and Pharmacology, Sapienza University of Rome,
Rome, Italy

C. Marchetti · G. Migliorati
Department of Clinical and Experimental Medicine,
University of Perugia,
Perugia, Italy

E. Castigli
Department of Cellular and Environmental Biology,
University of Perugia,
Perugia, Italy

Introduction

Cancer cells generally exhibit an increased glycolysis for energy generation, associated with impairment of mitochondrial respiration and enhanced resistance to mitochondrial apoptosis (Joy et al. 2003; Beckner et al. 2005; Kroemer 2006). In the presence of mitochondrial inhibitors, melanoma and glioma cells maintain their ability to migrate using the ATP produced only by glycolysis (Beckner et al.

1990). Under anaerobic conditions, lactate dehydrogenase supports glycolysis by regenerating NAD, thus producing lactate that must be eliminated. In astrocytes, lactate is released and utilized by neurons as an energy substrate. Alternatively, the excess lactate may be stored through gluconeogenesis and glycogen synthesis (Dringen et al. 1993; Bernard-Hèlary et al. 2002). Malignant gliomas develop high adaptability to anaerobic conditions through biochemical instruments that increase the metabolic rate of glycolysis. However, suppression of mitochondrial respiration to force maximal reliance on glycolysis does not result in lactate overproduction. Inactivating mutations of PTEN (Phosphatase and Tensin homolog) in these cells are responsible for up-regulation of the phosphatidylinositol-3-kinase pathway, resulting in dephosphorylation and activation of glycogen synthase. This mechanism allows cells to remove the lactate carbon skeleton via temporary incorporation into glycogen (Beckner et al. 2005).

The biochemical differences between normal and cancer cells in metabolic pathways, particularly the increased dependence on glycolysis for ATP generation, have provided new therapeutical approaches that selectively attack tumor cells. In many types of cancer cells the increased glucose consumption is supported by type II hexokinase overexpression. In these cells the enzyme suppresses cell death by binding to mitochondria through interaction with a voltage-dependent anion channel (VDAC1) that regulates the release of cytochrome c (cyt c) and apoptosis inducing factor (AIF) in the cytosol (Pastorino et al. 2005). Bromopyruvate, a potent type II hexokinase inhibitor, is a new targeted antiglycolytic agent and is a promising agent for cancer therapy (Pedersen 2007). Indeed, bromopyruvate causes regression of solid tumors by ATP depletion (Ko et al. 2004). In several tumor cell lines, the drug induces cell death, although with a variety of biochemical mechanisms (Xu et al. 2005; Kim et al. 2008; Yun et al. 2009; Pereira da Silva et al. 2009; Qin et al. 2010).

In glioblastoma, the most aggressive form of malignant brain tumors originating from glial cells and their precursors, defective cell-cycle checkpoints and activation of anti-apoptotic activities contribute to the altered proliferative behavior (Maher et al. 2001; Holland 2001). In the GL15 glioblastoma cell line, apoptosis was induced following an imbalanced control of cell cycle progression (Castigli et al. 2000, 2006). Impairment of mitochondrial functions, cyt c release outside mitochondria, and apoptosis were observed in palmitate-treated GL15 cells (Buratta et al. 2008). Decreased cardiolipin levels and alteration of its acyl-chain composition produced by the treatment were responsible for the weakening of cyt c binding to the inner mitochondrial membrane, thus favoring release of the protein outside mitochondria and triggering the apoptotic cascade.

In this work, we have dissected the respiratory process of GL15 cells by supplying the respiratory chain with selected substrates and using specific inhibitors of respiratory chain complexes. We observed that compared to brain mitochondria, oxygen consumption is lower in GL15 cells. The respiratory chain is mainly sustained by succinate and glycerophosphate through respiratory Complex II. Antiglycolytic bromopyruvate caused a dramatic decrease of cell reducing power, as well as depletion of ATP, collapse of mitochondrial membrane potential, and specific degradation of cyt c within mitochondria, targeting cells to death by mechanisms involving autophagy.

Materials and methods

Chemicals 5,5′,6,6′-tetrachloro-1,1′,3,3′-tetraethylbenzimidazolylcarbocyanine iodide (JC-1) was from Molecular Probes Europe BV. Digitonin, carbonyl cyanide 3-chlorophenylhydrazone (CCCP), rotenone, antimycin A, propidium iodide (PI), cytochrome c were from Fluka. 3-(4,5-dimethyl-thiazol-2-yl)-2,5-diphenyl tetrazolium bromide (MTT), N-Acetyl-Asp-Glu-Val-Asp-7-amido-4-trifluoromethylcoumarin (Ac-DEVD-AFC), 7-amino-4-trifluoro-methylcoumarin (AFC), caspase-3 inhibitor (Ac-DEVD-CHO), dihydroethidine (DHE), the ATP bioluminescence assay kit, 3-nitropropionate, menadione, and respiratory substrates were obtained from Sigma (Italy). Cyt c mouse monoclonal antibody, AIF goat polyclonal antibody, Bax rabbit polyclonal antibody, goat anti-mouse HRP-conjugated IgG, and rabbit anti-goat HRP-conjugated IgG were from Santa Cruz Biotechnology; LC3B rabbit polyclonal antibody, glyceraldehyde-3-phosphate dehydrogenase (GAPDH), β-actin, and β-tubulin mouse monoclonal antibodies were from Sigma; VDAC1 rabbit polyclonal antibody was from Calbiochem; glycogen synthase kinase-3 β (GSK-3β) (27C10) rabbit monoclonal antibody, which detects endogenous levels of total GSK-3β protein, phospho-GSK-3β (Ser9) rabbit antibody, which detects endogenous levels of GSK-3β only when phosphorylated at serine 9, the phospho-Akt (Ser473) rabbit monoclonal antibody, which detects endogenous levels of Akt only when phosphorylated at Ser473, and goat anti-rabbit HRP-conjugated IgG were from Cell Signaling Technology. The annexin V-FITC apoptosis detection kit was from eBioscience.

Cell culture and treatments GL15 glioblastoma cells were grown in Dulbecco's modified Eagle's medium (DMEM) supplemented with 10% heat-inactivated fetal bovine serum, 100 IU/ml penicillin G, 100 μg/ml streptomycin, 2 mM glutamine, and 1 mM sodium pyruvate. The cells were trypsinized, plated in 6-well plates (2×10^5 cells per

well), and incubated for 3 days at 37 °C in a 5% CO_2 humidified atmosphere to obtain semi-confluent cells. Medium was removed and cells were incubated for 18 h in serum-free DMEM in the presence of rotenone (10 μM), or NaN_3 (10 mM), or antimycin A (10 μM), or 3-nitropropionate (10 mM), or CCCP (10 μM). Where indicated, cells were incubated in the presence of a buffered solution of bromopyruvate (0–80 μM, pH 7.4) in the absence or presence of menadione (10 μM) or N-acetylcysteine (4 mM). Treatment of cells with 70 μM bromopyruvate produced cell detachment that was massive at 80 μM. Detached and trypsinized adherent cells were combined for subsequent analysis.

MTT reduction assay The metabolic reduction of 3-(4,5-dimethylthiazol-2-yl)-2,5-diphenyl tetrazolium bromide (MTT) (colorless) to formazan (blue) by cell dehydrogenases was evaluated. Cells were seeded in 96-well plates at a density of about 10^4 cells per well for the treatments described. After treatment, adherent cells were incubated 3 h with 0.5 mg/ml MTT and the formazan produced was solubilized with dimethyl sulfoxide. Absorbance at 570 nm was measured on an automated microtiter plate reader spectrophotometer.

Cell permeabilization Cells were resuspended in chilled buffer A containing 75 mM sucrose, 100 mM KCl, 10 mM KH_2PO_4, 5 mM $MgCl_2$, 0.5 mM EDTA, 20 mM Tris-HCl (pH 7.4), or B containing 300 mM sucrose, 4 mM KCl, 0.1 mM EDTA, 10 mM Hepes (pH 7.4). Digitonin (0.1%, w/v in buffer A or B) was added slowly to a final concentration of 0.1 mg/mg protein. After incubation for 10 min at 0 °C, cells were recovered by centrifugation (250× *g*, 10 min) and permeabilization was evaluated by propidium iodide (PI) staining of DNA. To this purpose, aliquots of cells were added to a cuvette containing buffer A (2 ml), PI was added to a final concentration of 10 μM, and fluorescence was monitored at 604 nm (λ_{exc} 535 nm). PI did not penetrate the plasma membrane of non-treated cells, as demonstrated by the lack of elicited fluorescence. In contrast, in digitonin-treated cells PI fluorescence reached values similar to that elicited in the presence of 0.2% THESIT detergent, indicating that permeabilization of all cells had occurred.

Respiratory activity Two types of experiments were performed. i) Intact cells were resuspended in a buffer containing 124 mM NaCl, 3 mM KCl, 1.8 mM $MgSO_4$, 1.6 mM $CaCl_2$, 1.25 mM NaH_2PO_4, 26 mM $NaHCO_3$, and 10 mM glucose (artificial glucose-containing cerebrospinal fluid), and incubated in the presence of inhibitors (NaN_3, 10 mM; antimycin A, 10 μM; rotenone, 3 μM; 3-nitropropionate, 10 mM, and CCCP 10 μM). ii) Cells were permeabilized in buffer A and resuspended in the same buffer in the presence of different respiratory substrates (3 mM) and inhibitors (NaN_3, 3 mM; antimycin A, 1.5 μM; rotenone, 1 μM). In both types of experiments cells were incubated for 30 min at 37 °C and the rate of oxygen consumption was determined as previously described (Macchioni et al. 2011). The oxygen content of the starting medium was normalized assuming a concentration of ~212 nmol/ml at 37 °C.

Analysis of mitochondrial proteins Cyt c, AIF, VDAC1, GAPDH and Bax were detected in intact cells using the

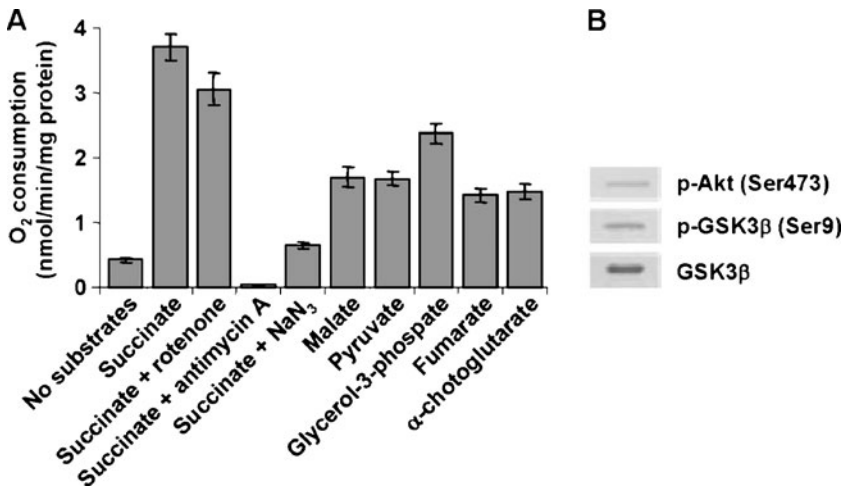

Fig. 1 Oxygen consumption rate of GL15 cells and GS3Kβ expression. **a** Permeabilized GL15 cells were resuspended in medium A in the presence of respiratory substrates and inhibitors, incubated for 30 min at 37 °C in a closed chamber, and oxygen consumption was immediately determined. The concentration of all substrates was 3 mM. The inhibitors were used at the following concentrations: rotenone, 1 μM; antimycin A, 1.5 μM; NaN_3, 3 mM. **b** Western blotting of GL15 cells grown in serum-free medium was performed using the p-Akt (Ser473), or the GS3Kβ, or the p-GS3Kβ (Ser9) antibodies

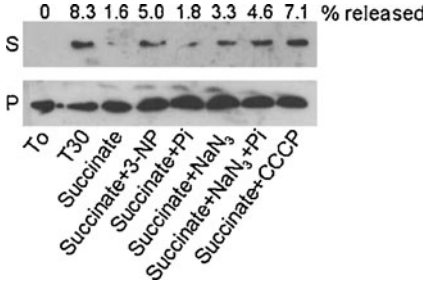

Fig. 2 Interaction of cyt c with the inner mitochondrial membrane in GL15 cells. Permeabilized GL15 cells were incubated for 30 min at 37 °C in low ionic strength medium (Buffer B) without succinate (T30) or with 3 mM succinate in the absence or presence of the indicated inhibitors (3-nitropropionate, 3-NP, 10 mM; NaN_3, 3 mM; CCCP, 5 μM) and 30 mM phosphate (Pi). To is zero time incubation. After centrifugation, released (supernatant, S) and retained (pellet, P) cyt c was assessed by Western blot. The amount of protein released into the supernatant was calculated as percentage of that in the pellet + supernatant combined. A representative Western blot of three independent experiments is shown

corresponding antibodies. To determine the release of cyt c and AIF into the cytosol from mitochondria, cells that had been incubated under different conditions were recovered from plates and permeabilized with digitonin in buffer B as described above. Aliquots were centrifuged (8,000×*g* for 10 min) and the supernatants were recovered. The pellets were resuspended in buffer B. Western blot analyses were performed in pellets and supernatants. Images of immunoblots were acquired using the VersaDoc 1000 imaging system and individual band densities were integrated by Quantity One software (BioRad).

Flow cytometry analyses For determination of mitochondrial membrane potential ($\Delta\psi_m$), the JC-1 probe (1 μM) was added to cells 30 min before the end of the incubation. Cells were recovered and changes of $\Delta\psi_m$ were analyzed using a FACScan flow cytometer (Beckman Coulter Epics XL-MCL) equipped with a focused argon laser. For complete depletion of $\Delta\psi_m$ (positive control), the mitochondrial uncoupler CCCP (5 μM) was used. Data were analyzed by a data management system (system II software, Beckman Coulter, UK). JC-1 fluorescence was detected as described (Piccotti et al. 2002), and green fluorescence (FL1) and red fluorescence (FL2) emission of particles were reported. Red energy distribution of cells was also related to forward (FS) and side (SS) light scatter, indices of particle size and granularity, respectively. To evaluate plasma membrane integrity after bromopyruvate treatment, GL15 cells were resuspended in isotonic buffer, stained with Annexin-V-FITC (1 μg/ml) plus PI (1 μg/ml), and analyzed by flow cytometry. In parallel experiments, flow cytometry analysis was performed in hypotonic solution containing PI (1 μg/ml). Cells incubated in the presence of 0.6 mM palmitate were used as a positive control for membrane permeabilization and DNA fragmentation (Buratta et al. 2008). To measure in situ O_2^- production, bromopyruvate-treated cells were incubated in the presence of 5 μM DHE and the oxidized fluorescent ethidine was monitored in the FL2 channel by flow cytometry at 530 nm (λ_{exc} 488 nm). A positive control was obtained by incubating cells with the free radical inducer menadione (10 μM).

Fig. 3 Effect of respiratory chain inhibitors on $\Delta\psi_m$ in GL15 cells. ▶ GL15 cells were incubated for 18 h in serum-free DMEM in the presence of rotenone, 3-nitropropionate (3-NP), antimycin A, NaN_3 or CCCP. Thirty min before the end of incubation cells were loaded with JC-1 probe (1 μM), then resuspended in buffer A. Dot plot of single GL15 cells and the percentage of cells within prefixed energy sectors (FL2 and FL1 channels) are shown. Red energy distribution of cells was also related to forward (FS) and side (SS) light scatter, indices of particle size and granularity, respectively. A representative experiment of four is shown

Cell death detection by ELISA Two assays were used. i) Necrosis assay. Determination of histone-associated DNA fragments, released in the culture medium by necrotic cells, was performed using the Cell Death Detection ELISA (PLUS) kit (ROCHE), according to instructions. ii) Apoptosis assay. The same kit was used to detect cytoplasmic nucleosomes in apoptotic cells. The results are expressed as percentage of optical density, resulting from the activity of peroxidase-conjugated anti-DNA-antibody complexed with cytoplasmic nucleosomes of treated cells, compared to the control.

Other methods The specific fluorogenic peptide substrate Ac-DEVD-AFC was used to determine caspase-3 activity as described (Buratta et al. 2008). ATP was measured using the ATP bioluminescence assay kit (Sigma), following the manufacturer's procedure.

Results

Oxygen consumption by GL15 cells a) Permeabilized cells. After permeabilization with digitonin, cells were incubated in medium A for 30 min at 37 °C in the presence of different substrates and respiratory chain inhibitors and oxygen content was evaluated immediately. Succinate and glycerophosphate fed the respiratory chain (Complex II) more efficiently than did the NAD-dependent substrates (Complex I) (Fig. 1a). NaN_3 and antimycin A, but not the Complex I inhibitor rotenone, blocked oxygen flux from succinate. *b*) Intact cells. Cells were resuspended in artificial glucose-containing cerebrospinal fluid and incubated for 30 min at 37 °C. Compared to permeabilized cells, the levels of oxygen consumption were low (about 0.5 nmol×mg $prot^{-1}$×min^{-1}), suggesting that the cytosolic compartment was involved mainly in energy supply.

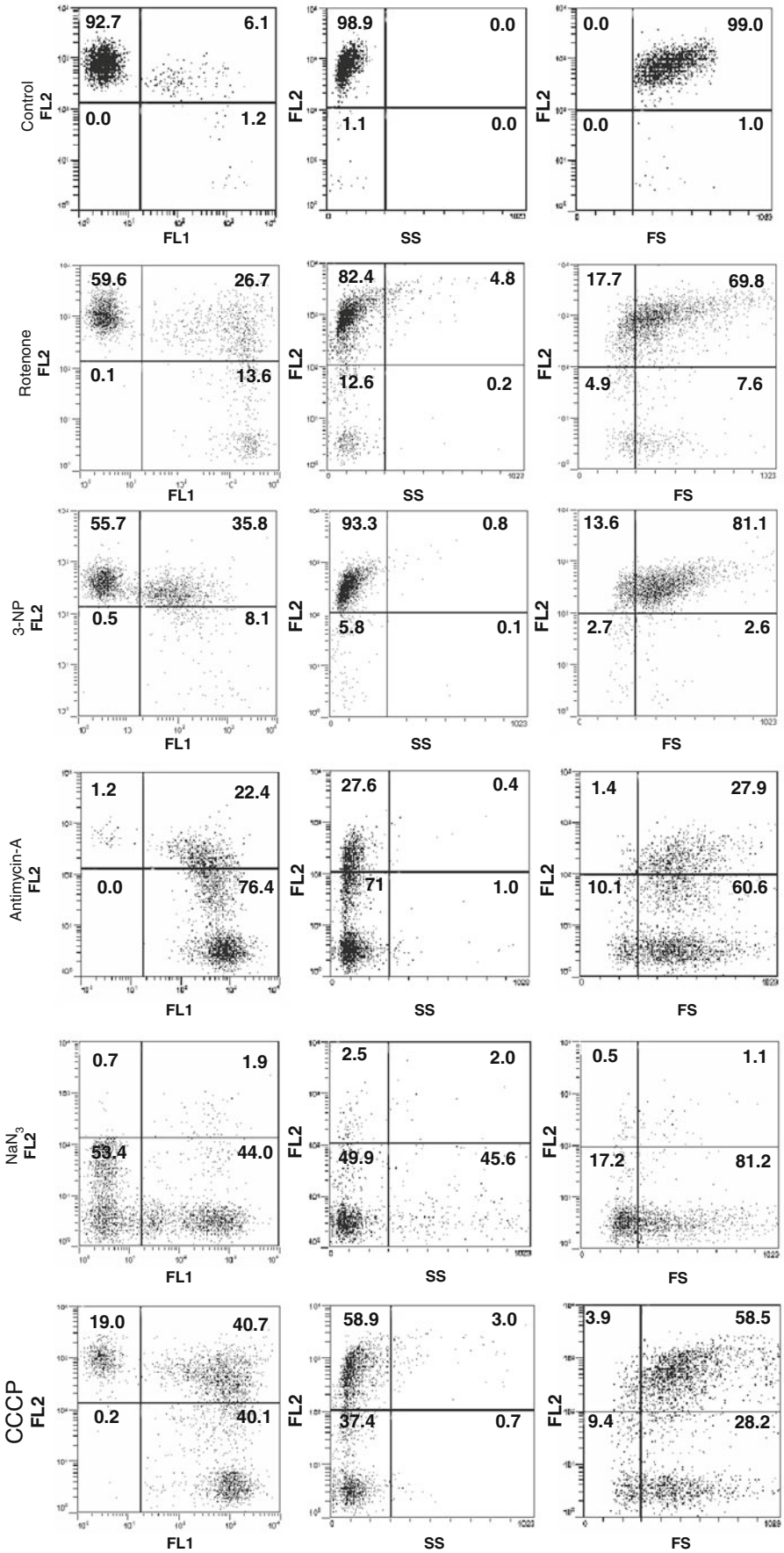
Control
FL2
92.7
6.1
0.0
1.2
FL1
98.9
0.0
1.1
0.0
SS
0.0
99.0
0.0
1.0
FS
Rotenone
59.6
26.7
0.1
13.6
82.4
4.8
12.6
0.2
17.7
69.8
4.9
7.6
3-NP
55.7
35.8
0.5
8.1
93.3
0.8
5.8
0.1
13.6
81.1
2.7
2.6
Antimycin-A
1.2
22.4
0.0
76.4
27.6
0.4
71
1.0
1.4
27.9
10.1
60.6
NaN3
0.7
1.9
53.4
44.0
2.5
2.0
49.9
45.6
0.5
1.1
17.2
81.2
CCCP
19.0
40.7
0.2
40.1
58.9
3.0
37.4
0.7
3.9
58.5
9.4
28.2

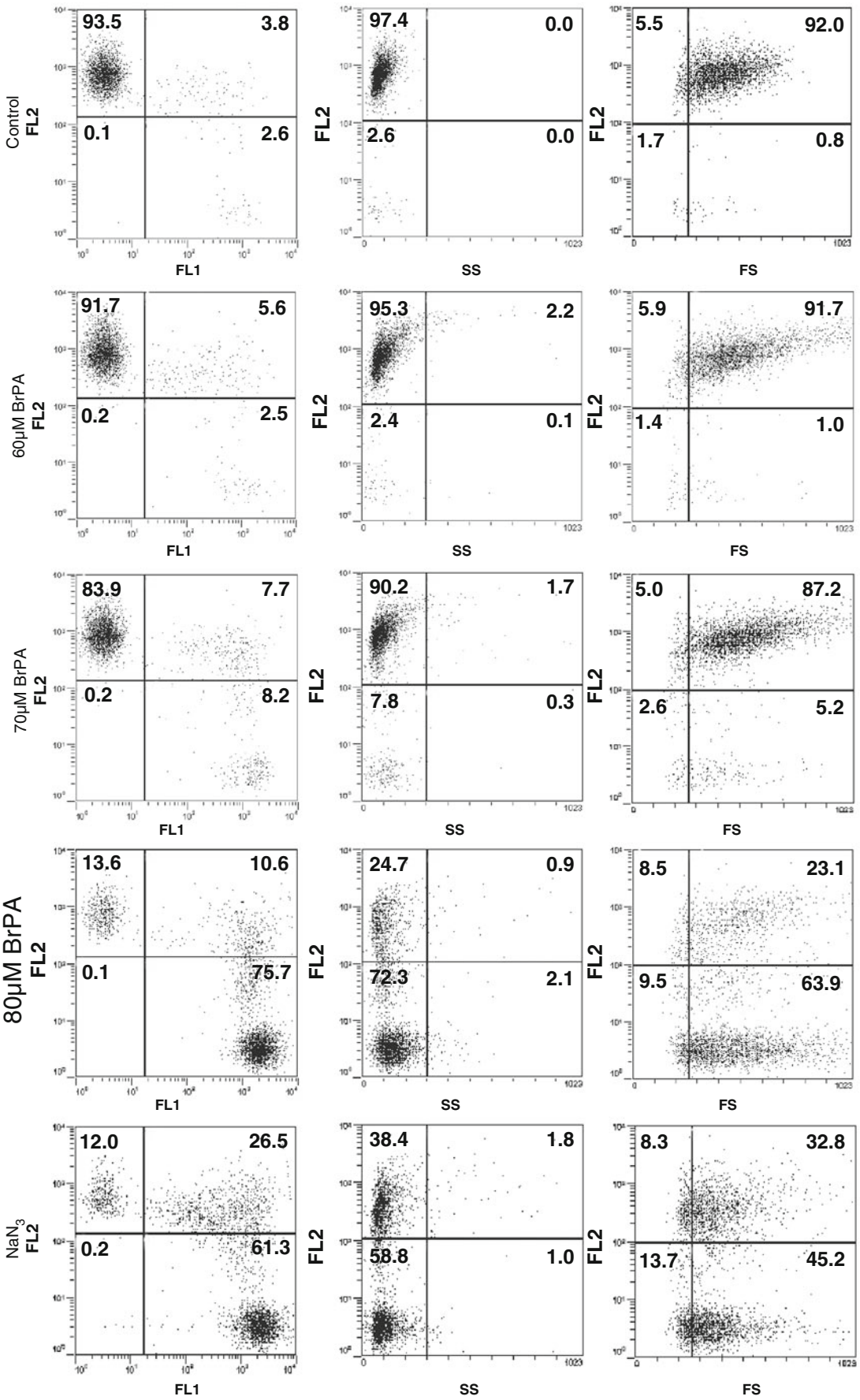
Control
FL2
93.5
3.8
0.1
2.6
FL1
97.4
0.0
2.6
0.0
FL2
SS
5.5
92.0
1.7
0.8
FL2
FS
60μM BrPA
FL2
91.7
5.6
0.2
2.5
FL1
95.3
2.2
2.4
0.1
FL2
SS
5.9
91.7
1.4
1.0
FL2
FS
70μM BrPA
FL2
83.9
7.7
0.2
8.2
FL1
90.2
1.7
7.8
0.3
FL2
SS
5.0
87.2
2.6
5.2
FL2
FS
80μM BrPA
FL2
13.6
10.6
0.1
75.7
FL1
24.7
0.9
72.3
2.1
FL2
SS
8.5
23.1
9.5
63.9
FL2
FS
NaN3
FL2
12.0
26.5
0.2
61.3
FL1
38.4
1.8
58.8
1.0
FL2
SS
8.3
32.8
13.7
45.2
FL2
FS

◀ **Fig. 4** $\Delta\psi_m$ of bromopyruvate-treated GL15 cells. GL15 cells were incubated for 18 h in serum-free DMEM in the presence of increasing bromopyruvate (BrPA) concentrations. Thirty min before the end of incubation cells were loaded with JC-1 probe (1 μM), then resuspended in buffer A and analyzed as described for Fig. 3. $\Delta\psi_m$ was completely depleted with 10 mM NaN_3 (positive control). One representative experiment of four is shown

We investigated whether this observed suppression of mitochondrial respiration in GL15 cells was balanced by the activation of glycogen synthase, considering that the PI3K/Akt pathway is constitutively activated in these cells (Sciaccaluga et al. 2010). Indeed, Fig. 1b shows that Akt phosphorylation at Ser473 is responsible for activation of this pathway, leading to the constitutive inhibition of GSK3β via phosphorylation of Ser9, thus favoring the dephosphorylated form of glycogen synthase.

Interactions of cyt c in GL15 mitochondria In mitochondria, most cyt c is membrane bound with only a small pool interacting tightly, the rest being loosely bound. In brain mitochondria, about 30% of the loosely bound protein can be detached and released from mitochondria by 30 mM phosphate, which interferes with the hydrophilic component of cyt c-cardiolipin interactions (Piccotti et al. 2002). To evaluate cyt c hydrophobic/hydrophilic interaction balance, permeabilized GL15 cells were incubated for 30 min at 37 °C in medium of low ionic strength under different respiratory conditions. After centrifugation, the released (supernatant) and retained (pellet) cyt c was determined. In the presence of succinate, only trace amounts of cyt c were released, and the release of cyt c increased in the absence of succinate or in the presence of inhibitors (Fig. 2). In contrast to brain mitochondria, 30 mM phosphate did not enhance cyt c release, indicating that in GL15 cells the hydrophobic component of cyt c-cardiolipin interactions is stronger than in neural mitochondria.

$\Delta\psi_m$ of GL15 mitochondria: effect of respiratory chain inhibitors GL15 cells were incubated in the presence or absence of respiratory chain inhibitors, loaded with JC-1, and submitted to flow cytometric analysis. In Fig. 3, each dot represents a single cell analyzed for its green- (FL1) and orange- (FL2) associated fluorescence. Under control conditions, ~80% of cells exhibited high $\Delta\psi_m$, as indicated by orange fluorescence. Orange fluorescence shifted to green following incubation of cells with the Complex III inhibitor antimycin A, whereas the Complex IV inhibitor NaN_3 collapsed $\Delta\psi_m$; both inhibitors exceeded the uncoupling effect of CCCP. In the presence of the Complex II inhibitor 3-nitropropionate, ~40% of cells moved to green fluorescence, whereas the orange fluorescence of the remaining 58% cells decreased, compared to control. On the other hand, the Complex I inhibitor rotenone did not affect $\Delta\psi_m$ significantly, since ~60% of the cells maintained a high $\Delta\psi_m$. Size (FS) and complexity/granularity (SS) were also determined after each treatment. FS and SS were deeply influenced in antimycin A- and NaN_3-treated cells compared to control. Rotenone and nitropropionate had no effect (Fig. 3).

Effects of bromopyruvate treatment of GL15 cells GL15 cells were treated with bromopyruvate (0–80 μM) for 18 h and analyzed by flow cytometry, following JC-1 incorporation. The distribution of neither $\Delta\psi_m$ nor FS and SS was affected by bromopyruvate in the 0–60 μM range (Fig. 4). $\Delta\psi_m$ collapse began with 70 μM bromopyruvate concentration, involving a significant pool of GL15 cells (about 8%). $\Delta\psi_m$ collapsed in all cells when the bromopyruvate concentration reached 80 μM. ATP levels did not change up to 60 μM bromopyruvate concentration and reached ~58% and ~7% of the control in 70 μM and 80 μM bromopyruvate-treated cells, respectively.

Concomitant with the drop in $\Delta\psi_m$ and the decrease in cellular ATP, a loss of cyt c in the cell was observed (Fig. 5a). Analysis of other mitochondrial proteins showed decreased expression of Bax and, to a lesser extent, of AIF, whereas the VDAC1 protein was unaffected. At the same time, cytosolic glyceraldeyde-3-phosphate dehydrogenase and the housekeeping proteins β-tubulin and β-actin were unaltered (Fig. 5a). Moreover, in bromopyruvate-treated cells, cyt c and AIF were not detected in the supernatant after permeabilization and centrifugation, suggesting that they were not released into the cytosol (Fig. 5b). It should

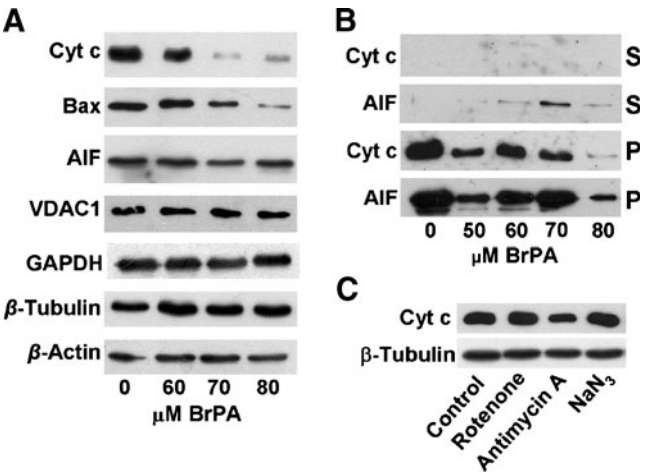

Fig. 5 Effect of bromopyruvate and inhibitors on mitochondrial and cytosolic proteins. GL15 cells were incubated for 18 h in serum-free DMEM in the presence of increasing bromopyruvate (BrPA) concentrations or inhibitors. Western blotting was performed in intact cells (panels **a** and **c**) or in pellets (P) and supernatants (S) of digitonin permeabilized cells (panel **b**). Representative blots of four independent experiments are shown

be noted that treatment of GL15 cells with respiratory chain inhibitors did not release cyt c from mitochondria (not shown) or increase its degradation, with the exception of antimycin A, which decreased intramitochondrial cyt c (Fig. 5c). No caspase-3 activity was detected under any condition (not shown). Thus, the activation of this pathway is excluded.

ATP depletion is a hallmark of necrosis. Thus, induction of necrosis/apoptosis was investigated in bromopyruvate-treated cells. Cells were resuspended in isotonic medium in the presence of annexin V-FITC and/or PI and analyzed by cytofluorimetry. Dot plot distribution of particles in the diagram reporting annexin V-FITC fluorescence (FL1) versus PI fluorescence (FL3) indicated that neither phosphatidylserine exposure nor plasma membrane permeabilization had occurred in control or bromopyruvate-treated cells (Fig. 6a). Moreover, DNA was not fragmented, as indicated by the lack of a decrease in PI fluorescence in treated, compared to control cells resuspended in hypotonic medium (Fig. 6b). A positive control, performed by incubating the cells with 0.6 mM palmitate (Buratta et al. 2008), indicated that both permeabilization and DNA fragmentation occurred under these conditions (Fig. 6a and b). The lack of apoptosis or necrosis induction by 80 μM bromopyruvate was confirmed by the ELISA cell death detection method, performed after 3 days of treatment

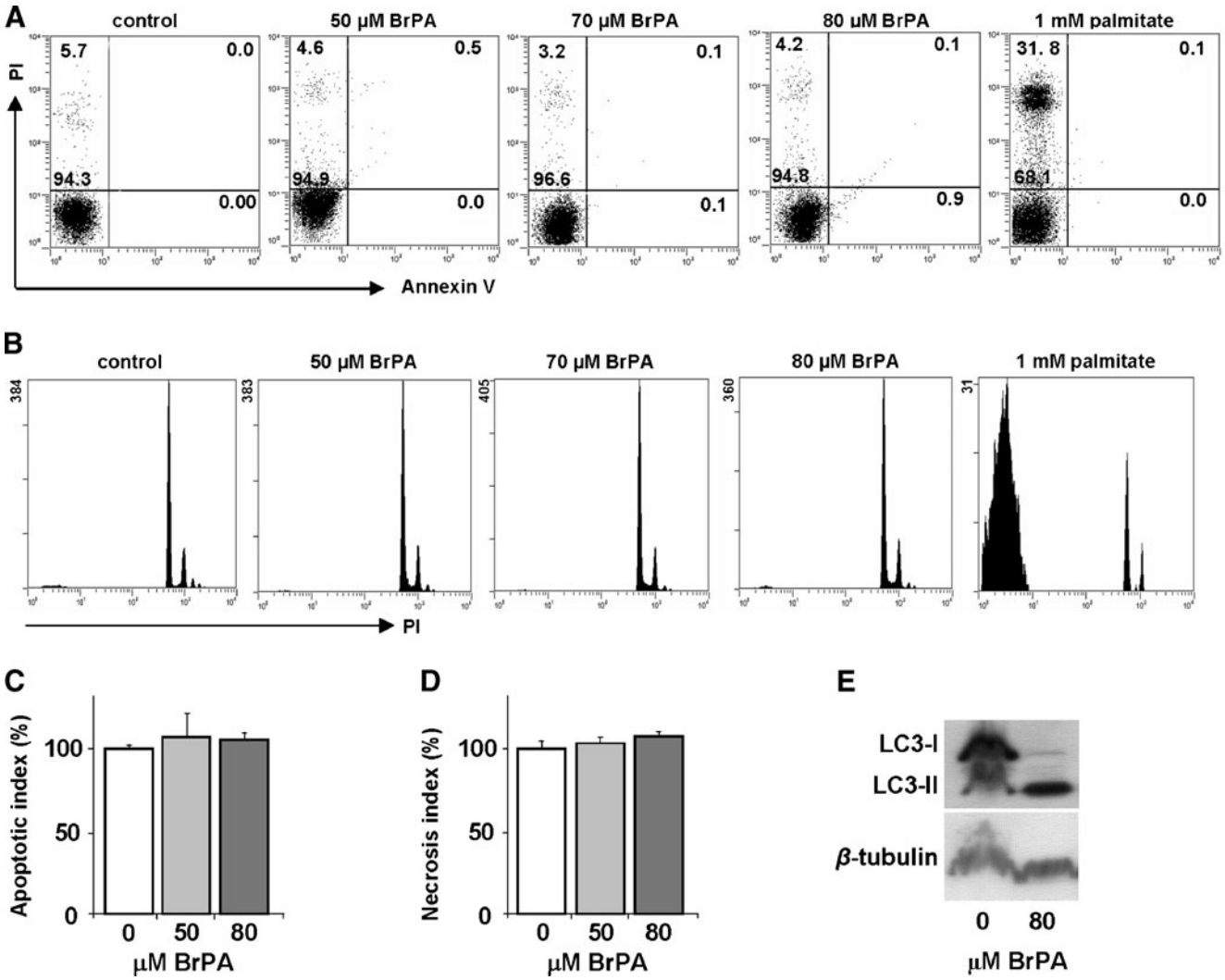

Fig. 6 Bromopyruvate-treated GL15 cells: analysis of phosphatidylserine exposure, PI permeabilization, DNA fragmentation, and autophagy. GL15 cells were incubated for 18 h in serum-free DMEM in the presence of increasing concentrations of bromopyruvate (BrPA). **a** Cells were resuspended in isotonic medium (Buffer B) in the presence of annexin V-FITC and PI, and analyzed by cytofluorimetry. A dot plot distribution of particles reporting annexin V-FITC fluorescence (FL1) versus PI fluorescence (FL3) is shown. **b** Cells were resuspended in hypotonic medium in the presence of PI. PI fluorescence (FL3) is reported. In each experiment, cells treated with 0.6 mM palmitate acted as positive controls for both cell permeabilization and DNA fragmentation. **c** Apoptotic index. **d** Necrosis index. **e** Immunoblots of the autophagy marker microtubule-associated protein light chain 3 (LC3) indicating the conversion of the free LC3-I form to its lipidated, autophagosome-associated LC3-II form. Representative experiments out of four are shown

(Fig. 6c and d). However, immunoblots of bromopyruvate-treated cells for the autophagy marker microtubule-associated protein light chain 3 (LC3) indicated the conversion of the free LC3-I form to its lipidated, autophagosome-associated LC3-II form (Fig. 6e).

Reducing potential of GL15 cells: effect of respiratory chain inhibitors and bromopyruvate The extent of MTT reduction was determined as an index of reducing cellular metabolic activities. At the mitochondrial level, MTT reduction takes place at distinct sites of the electron transport chain (Liu et al. 2002). A decrease of MTT reduction activity was observed upon blocking the respiratory chain downstream Complex I. Thus, in the presence of 3-nitropropionate (Complex II), antimycin A (Complex III), NaN_3 (Complex IV), and the uncoupling agent CCCP, ~66%, 74%, 37%, and 85% activity was detected, respectively (Fig. 7a). Rotenone, an inhibitor of Complex I, did not affect MTT reduction, indicating that Complex I does not contribute to the formation of the reducing potential. The antiglycolytic compound bromopyruvate decreased MTT reduction at concentrations at and above 60 μM (Fig. 7b). Massive detachment of dead cells occurred with 80 μM bromopyruvate concentration, consistent with the significant decrease of the reducing potential of adherent cells.

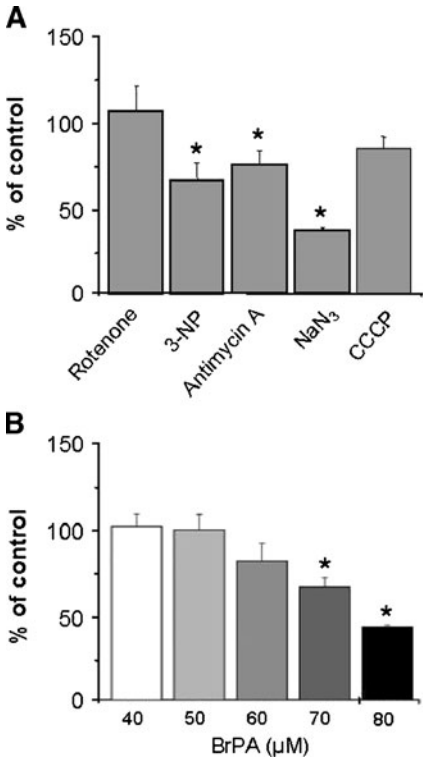

Fig. 7 Effect of respiratory inhibitors and bromopyruvate on GL15 cell-reducing potential. GL15 cells were incubated for 18 h in serum-free DMEM in the presence of rotenone, 3-nitropropionate (3-NP), antimycin A, NaN_3 or CCCP (panel **a**) or in the presence of bromopyruvate (BrPA) (panel **b**). MTT reduction of adherent cells was measured. Data are expressed as the percent of the mean absorbance of the control (570 nm). * Significance reached, $p<0.01$ (Student's t-test)

Cyt c degradation: correlation with free radicals production The decrease in MTT reduction activity caused by bromopyruvate suggests that the redox equilibrium in the cell was altered. Therefore, we evaluated whether bromopyruvate-mediated cell death was linked to free radical generation. Figure 8 shows an increase of FL2 channel fluorescence in response to DHE oxidation in GL15 cells incubated with increasing bromopyruvate concentrations, indicating free radical production. Cells treated with the free radical inducer menadione were the positive control of superoxide anion generation, which was counteracted by the scavenging property of N-acetylcysteine. A tight correlation was observed between cyt c degradation and free radical production in menadione-treated cells, since cyt c degradation was reversed by N-acetylcysteine (Fig. 9). In addition, it should be considered that the ROS inducer antimycin A exerted an effect similar to menadione on cyt c (see Fig. 5c). Cyt c degradation was not observed when bromopyruvate-treated cells were co-incubated with N-acetylcysteine. However, it is noteworthy that bromopyruvate acts also as an alkylating agent towards the -SH groups of N-acetylcysteine.

Discussion

It has been long recognized that cancer cells may have alterations in mitochondria, leading to increased glycolysis, even in the presence of oxygen. Thus, in this study bioenergetics and metabolic features of GL15 glioblastoma cells have been investigated. First, we found that oxygen consumption is restricted to the use of substrates feeding the respiratory chain Complex II. Second, binding of cyt c with the inner mitochondrial membrane is characterized by strong hydrophobic interactions. Third, inhibition of mitochondrial and glycolytic ATP production with bromopyruvate causes collapse of mitochondrial $\Delta\psi_m$, loss of cell viability, and specific cyt c degradation within mitochondria.

In the normal cell an efficient mitochondrial oxidative phosphorylation, supported by elevated oxygen consumption, is required to meet the high energy needs. In contrast, tumor cells rely preferentially on anaerobic glycolysis for ATP generation, even when oxygen is available (Warburg 1956; Pedersen 2007). Evidence of the low propensity of GL15 cells to respire comes from the low respiratory rate in the presence of a glucose-based medium. In order to select respiratory substrates that were able to supply the respira-

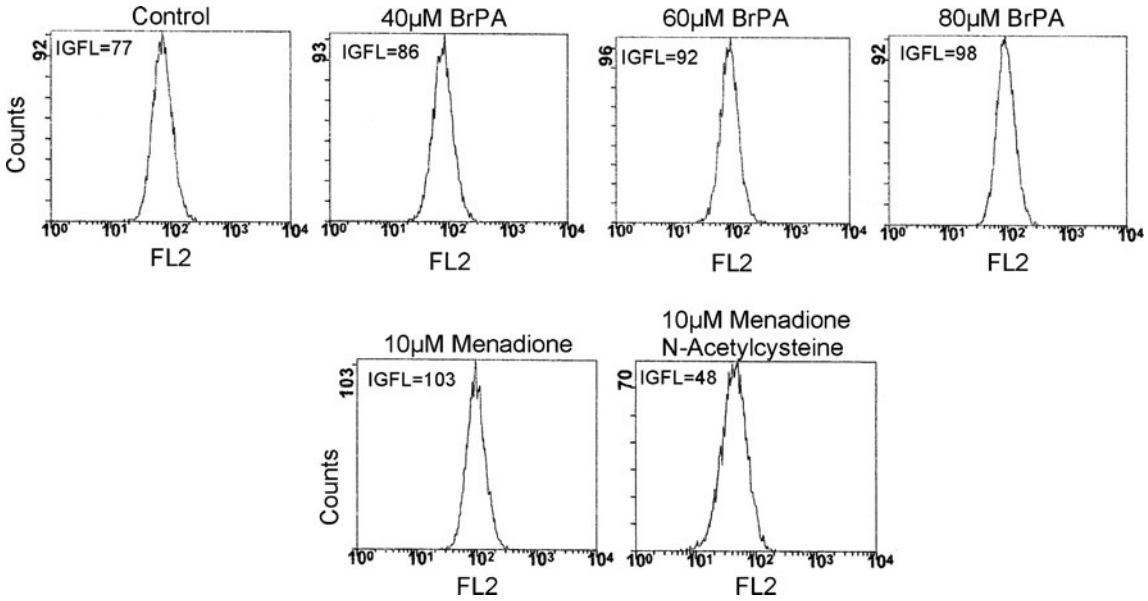

Fig. 8 Detection of superoxide anion in bromopyruvate-treated GL15 cells. After treatment with bromopyruvate (BrPA), cells were incubated in the presence of 5 μM dihydroethidine for 15 min at 37 °C and cellular O_2^- was analyzed by cytofluorimetry. Cells treated with the free radical inducer menadione (10 μM) acted as a positive control, whereas N-acetylcysteine was used as oxygen radical scavenger. The mean value of the integral of the fluorescence (IGFL) is reported. A representative experiment of three is shown

tory chain, cells were permeabilized and substrates were added in the incubation medium. The data indicate that Complex II substrates are the preferred substrates (Fig. 1a).

The low level of oxygen consumption of GL15 cells meets their dependence on anaerobic glycolysis to support the energetic need, although glucose-derived carbon skeleton should also feed the respiratory chain to create $\Delta\psi_m$ (Fig. 3, control). To assess the electron flux along the respiratory chain, respiratory complexes were selectively inhibited. Inhibition of Complex III with antimycin A, or inhibition of the downstream Complex IV with NaN_3, resulted in $\Delta\psi_m$ collapse, suggesting that all the reducing equivalents routing from Complexes I and II were blocked. The entrance of FAD-dependent reducing equivalents at the level of Complex II was also affected after inhibition with nitropropionate. No effect was elicited by rotenone, indicating that the $\Delta\psi_m$ is not supported by electrons routing through Complex I. It can be inferred that in GL15 cells Complex I is scarcely operative, confirming that only FAD-dependent substrates are preferred to support the $\Delta\psi_m$ (Fig. 1a). Despite the complete collapse of the $\Delta\psi_m$, cells treated with antimycin A, NaN_3, or CCCP were still sustained by reducing potential, as shown by MTT reduction, indicating the role of cytosolic pathways in energy supply (Fig. 7a).

Inhibition of glycolysis represents a new approach for targeting energy production in cancer cells affected by mitochondrial defects. The alkylating agent bromopyruvate inhibits ATP production via both mitochondrial and glycolytic pathways in cancer cells while not altering normal cells (Ko et al. 2001; Geschwind et al. 2002, 2004; Pedersen 2007). In GL15 cells bromopyruvate was effective at a concentration of 80 μM, producing a decrease in $\Delta\psi_m$, ATP, and MTT (Figs. 4 and 7b). No pathways indicative of apoptosis or cellular necrosis were observed (Fig. 6). However, the detection of the autophagosome-associated form of LC3 (LC3-II) indicated that an autophagic process was triggered (Fig. 6e). This

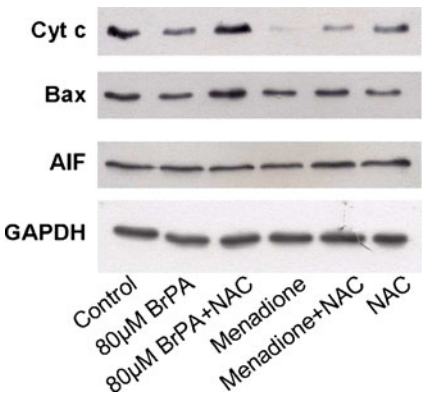

Fig. 9 Correlation between cyt c degradation and free radical production. GL15 cells were incubated for 18 h in serum-free DMEM in the presence of bromopyruvate (80 μM) or menadione (10 μM). N-acetylcysteine (NAC) (4 mM) was used as oxygen radical scavenger. Western blotting of cyt c, BAX, AIF, and glyceraldehyde-3-phosphate dehydrogenase (GAPDH) was performed in intact cells. A representative experiment of three is shown

result is in agreement with studies showing that glioblastoma cells are less resistant than other cells to autophagy-inducing therapies (Ito et al. 2006; Lefranc et al. 2007; Jiang et al. 2007).

Bromopyruvate-mediated cell death has been linked to free radical generation (Ganapathy-Kanniappan et al. 2010). In mitochondria, H_2O_2 produced from O_2^- by superoxide dismutase feeds the cyt c peroxidase activity responsible for cardiolipin oxidation (Huang et al. 2008). Indeed, cyt c acquires peroxidase activity when tightly bound to cardiolipin (Kagan et al. 2004), an event followed by cyt c release from mitochondria (Kagan et al. 2005; Huang et al. 2008; Macchioni et al. 2011). In GL15 cells, the hydrophobic (tightly bound)/hydrophilic (loosely bound) balance between cyt c-cardiolipin interactions is in favor of the hydrophobic component (Fig. 2). We found increased superoxide anion O_2^- in bromopyruvate treated GL15 cells (Fig. 8) that was not accompanied by cyt c release into the cytosolic compartment (Fig. 5b). In addition, loss of cyt c from mitochondria occurred, whereas other mitochondrial proteins, such as AIF and VDAC1, but not Bax, were unaffected (Fig. 5a). Therefore, mechanisms other than the ROS-mediated release of pro-apoptotic factors in bromopyruvate-treated GL15 cells must be operative.

Protein oxidation by ROS leads to modification of amino acid side-chains (Babusikova et al. 2007). In mitochondria, oxidative insult produces structural changes of proteins that mark them for degradation by intramitochondrial proteases (Bota and Davies 2001; Koppen and Langer 2007). Moreover, destabilization of cyt c helices results in increased susceptibility to proteolysis (Groves et al. 2004). We hypothesize that cyt c disappearance within mitochondria in bromopyruvate-treated cells may be the result of activated proteolytic activities in mitochondria, following an oxidative insult towards the protein. Indeed, the reducing power of N-acetylcysteine counteracted the degradation of cyt c in GL15 cells treated with the free radical inducer menadione (Fig. 9). The decrease of Bax, a pro-apoptotic member of the Bcl-2 family that favors cyt c release by mediating the permeabilization of the outer mitochondrial membrane (Gogvadze and Zhivotovsky 2007) (Fig. 5a), supports the hypothesis of a metabolic scenario involving intra-mitochondrial cyt c degradation.

A peculiar feature of GL15 cells is the tight binding of cyt c to the inner mitochondrial membrane that enables cells to escape the cyt c-triggered apoptotic pathway. GL15 cell starvation produced by bromopyruvate forces these cells to switch to respiration for their energy supply. Thus, cyt c is targeted for degradation, possibly due to acquired peroxidase activity. This process is specific and impairs the apoptotic cyt c cascade, although cells are committed to die.

Acknowledgements We are grateful to Professor Jean Vance, University of Alberta, Edmonton, Canada for the critical reading of this manuscript. This work was supported by Fondazione CARIT, Progetti di Sviluppo 2008, Terni, Italy and by Fondazione Cassa di Risparmio di Perugia (Progetto 2010.020.0132), Perugia, Italy. We thank Carlo Ricci for skillful technical assistance.

References

Babusikova E, Hatok J, Dobrota D, Kaplan P (2007) Neurochem Res 32:1351–1356
Beckner ME, Stracke ML, Liotta LA, Schiffmann E (1990) J Natl Cancer Inst 82:1836–1840
Beckner ME, Gobbel GT, Abounader R, Burovic F, Agostino NR, Laterra J, Pollack IF (2005) Lab Invest 85:1457–1470
Bernard-Hèlary K, Ardourel M, Magistretti P, Hévor T, Cloix JF (2002) Glia 37:379–382
Bota DA, Davies KJA (2001) Mitochondrion 1:33–49
Buratta M, Castigli E, Sciaccaluga M, Pellegrino RM, Spinozzi F, Roberti R, Corazzi L (2008) J Neurochem 105:1019–1031
Castigli E, Arcuri C, Giovagnoli L, Luciani R, Giovagnoli L, Secca T, Gianfranceschi GL, Bocchini V (2000) Am J Physiol Cell Physiol 279:C2043–C2049
Castigli E, Sciaccaluga M, Schiavoni G, Brozzi F, Fabiani R, Gorello P, Gianfranceschi GL (2006) Oncol Rep 15:463–470
Dringen R, Gebhardt R, Hamprecht B (1993) Brain Res 623:208–214
Ganapathy-Kanniappan S, Vali M, Kunjithapatham R, Buijs M, Syed LH, Rao PP, Ota S, Kwak BK, Loffroy R, Geschwind JF (2010) Curr Pharm Biotechnol 11:510–517
Geschwind JF, Ko YH, Torbenson MS, Magee C, Pedersen PL (2002) Cancer Res 62:3909–3913
Geschwind JF, Georgiades CS, Ko YH, Pedersen PL (2004) Expert Rev Anticancer Ther 4:449–457
Gogvadze V, Zhivotovsky B (2007) J Bioenerg Biomembr 39:23–30
Groves K, Wilson AJ, Hamilton AD (2004) J Am Chem Soc 126:12833–12842
Holland EC (2001) Nat Rev Genet 2:120–129
Huang Z, Jiang J, Tyurin VA, Zhao Q, Mnuskin A, Ren J, Belikova NA, Feng W, Kurnikov IV, Kagan VE (2008) Free Radic Biol Med 44:1935–1944
Ito H, Aoki H, Kühnel F, Kondo Y, Kubicka S, Wirth T, Iwado E, Iwamaru A, Fujiwara K, Hess KR, Lang FF, Sawaya R, Kondo S (2006) J Natl Cancer Inst 98:625–636
Jiang H, Gomez-Manzano C, Aoki H, Alonso MM, Kondo S, McCormick F, Xu J, Kondo Y, Bekele BN, Colman H, Lang FF, Fueyo J (2007) J Natl Cancer Inst 99:1410–1414
Joy AM, Beaudry CE, Tran NL, Ponce FA, Holz DR, Demuth T, Berens ME (2003) J Cell Sci 116:4409–4417
Kagan VE, Borisenko GG, Tyurina YY, Tyurin VA, Jiang J, Potapovich AI, Kini V, Amoscato AA, Fujii Y (2004) Free Radic Biol Med 37:1963–1985
Kagan VE, Tyurin VA, Jiang J, Tyurina YY, Ritov VB, Amoscato AA, Osipov AN, Belikova NA, Kapralov AA, Kini V, Vlasova II, Zhao Q, Zou M, Di P, Svistunenko DA, Kurnikov IV, Borisenko GG (2005) Nat Chem Biol 1:223–232
Kim JS, Ahn KJ, Kim JA, Kim HM, Lee JD, Lee JM, Kim SJ, Park JH (2008) J Bioenerg Biomembr 40:607–618
Ko YH, Pedersen PL, Geschwind JF (2001) Cancer Lett 173:83–91
Ko YH, Smith BL, Wang Y, Pomper MG, Rini DA, Torbenson MS, Hullihen J, Pedersen PL (2004) Biochem Biophys Res Commun 324:269–275
Koppen M, Langer T (2007) Crit Rev Biochem Mol Biol 42:221–242
Kroemer G (2006) Oncogene 25:4630–4632
Lefranc F, Facchini V, Kiss R (2007) Oncologist 12:1395–1403

Liu Y, Fiskum G, Schubert D (2002) J Neurochem 80:780–787
Macchioni L, Davidescu M, Mannucci R, Francescangeli E, Nicoletti I, Roberti R, Corazzi L (2011) Biochim Biophys Acta 1811:203–208
Maher EA, Furnari FB, Bachoo RM, Rowitch DH, Louis DN, Cavenee WK, DePinho RA (2001) Genes Dev 15:1311–1333
Pastorino JG, Hoek JB, Shulga N (2005) Cancer Res 65:10545–10554
Pedersen PL (2007) J Bioenerg Biomembr 39:211–222
Pereira da Silva AP, El-Bacha T, Kyaw N, dos Santos RS, da Silva WS, Almeida FCL, Da Poian AT, Galina A (2009) Biochem J 417:717–726
Piccotti L, Marchetti C, Migliorati G, Roberti R, Corazzi L (2002) J Biol Chem 277:12075–12081
Qin J-Z, Xin H, Nickoloff BJ (2010) Biochem Biophys Res Commun 396:495–500
Sciaccaluga M, Fioretti B, Catacuzzeno L, Pagani F, Bertollini C, Rosito M, Catalano M, D'Alessandro G, Santoro A, Cantore G, Ragozzino D, Castigli E, Franciolini F, Limatola C (2010) Am J Physiol Cell Physiol 299:C175–184
Warburg O (1956) Science 123:309–314
Xu R-H, Pelicano H, Zhou Y, Carew JS, Feng L, Bhalla KN, Keating MJ, Huang P (2005) Cancer Res 65:613–621
Yun J, Rago C, Cheong I, Pagliarini R, Angenendt P, Rajagopalan H, Schmidt K, Willson JK, Markowitz S, Zhou S, Diaz LA Jr, Velculescu VE, Lengauer C, Kinzler KW, Vogelstein B, Papadopoulos N (2009) Science 325:1555–1559